S**upporting Information** for paper entitled "Mesoscopic interaction potential for carbon nanotubes of arbitrary length and orientation" by Alexey N. Volkov and Leonid V. Zhigilei

## S1. Numerical Implementation of the Approximate Tubular Potential

One of the main areas of prospective applications of the approximate tubular potential is in mesoscopic dynamic simulations of system consisting of a large number of interacting nanotubes (e.g. see Section 4). To make such simulations possible, the tubular potential should be implemented in a computer code capable of fast and accurate evaluation of interaction energies and forces acting on segments of the nanotubes. The efficiency of the evaluation of the forces and energies can be significantly improved by recording the functions necessary for calculation of the tubular potential in one- and two-dimensional tables and using interpolation of the tabulated values during the simulations. Similar approach is commonly used in atomistic molecular dynamics simulations, where the use of tables has been shown to significantly speed up the calculation of interatomic potentials and forces.[S1] In the tubular potential given by eqs 25 and 39, the use of tables for potential functions $u_{\infty\|}(h)$, $u_{e\|}(h,\xi)$, and $\Phi(h,\zeta)$ is found to bring significant computational benefits, whereas functions $\Gamma(h,\alpha)$, $\Omega(\alpha)$, $\Theta(\alpha)$, and $\zeta_{\min}(h)$ can be either tabulated or evaluated analytically.

The implementation of the tubular potential in a computer code should account for specific mathematical properties of the functions defining the potential. In particular, special care should be taken in the case of almost parallel nanotubes, when $\sin\alpha \to 0$ and the right part of eq 25 has an indeterminate form. Complex definitional domains of functions $\Phi(h,\zeta)$ and $u_{e\|}(h,\xi)$ and large gradients of these functions in parts of their domains require application of special computational procedures aimed at minimization of errors in evaluation of the functions and their derivatives. The ultimate criteria of the appropriate implementation of the tubular potential are (1) the computational efficiency of the calculation of energies and forces acting on nanotubes and (2) an acceptable accuracy of the total energy conservation in a simulation of an isolated system in which the mesoscopic dynamics is governed by internal potential forces. Below we briefly summarize our experience in the numerical implementation of the approximate tubular potential.

The tabulation of functions $u_{\infty\|}(h)$, $u_{e\|}(h,\xi)$, $\Phi(h,\zeta)$ and their derivatives requires introduction of the domains of the functions that are relevant to non-bonding interactions among nanotubes in systems with arbitrary (but physically reasonable) geometric arrangements of CNT segments. The natural choice of the boundaries of the relevant domains is defined by the finite range of the interatomic potential given by eq 1. The cutoff distance for interatomic interactions, $r_c$, can be directly translated to the cutoffs distances in the mesoscopic interaction potential. In addition, we slightly reduce the domain of the functions to exclude small regions adjacent to singularities, where the functions attain very large values.

For function $u_{\infty\|}(h)$, we consider domain defined as $h \in [2R_T + \Delta_0, h_{\max}]$, where $h_{\max} = 2R_T + r_c$ and $\Delta_0$ is a small positive constant. In the calculations reported in this paper, the value of $\Delta_0$ is chosen to be 0.3 Å, which is much smaller than the equilibrium distance $r_0 = 2^{1/6}\sigma \approx 3.82$ Å of the interatomic potential given by eq 1. With the potential energy density at the lower boundary of the domain being as high as $4\times10^8$ eV/Å, we do not expect such inter-tube distances to be realized in a dynamic mesoscopic simulation performed under realistic conditions.

For function $u_{e\|}(h,\xi)$, the domain used in the calculations is schematically shown in Figure S1. Due to the cutoff of the interatomic potential, $u_{e\|}(h,\xi) = 0$ for $h > h_{\max}$ and

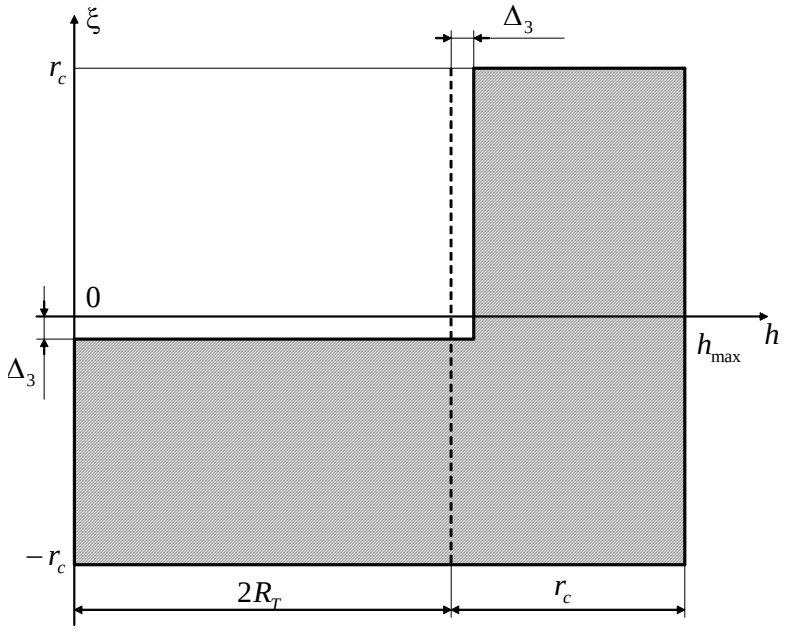


**Figure S1**. Sketch of the domain of the potential density function $u_{e\|}(h,\xi)$ used in the implementation of the tubular potential in the mesoscopic dynamic model. The domain of the function is shown by the gray area.

$u_{e\|}(h,\xi) = u_{\infty\|}(h)$ for $|\xi| \geq r_c$, making it unnecessary to define $u_{e\|}(h,\xi)$ for these geometric conditions. In addition, the region where $h \leq 2R_T$ and $\xi > 0$ should be excluded as it corresponds to the intersection of the surfaces of the segment and the nanotube. The domain of the potential density $u_{e\|}(h,\xi)$, therefore, can be defined as a combination of two rectangular parts: $[0,h_{\max}]\times[-r_c,0)$ and $(2R_T,h_{\max}]\times[0,r_c]$. In order to exclude regions of the domain with very high values of $u_{e\|}(h,\xi)$ (which correspond to surfaces of interacting nanotubes being "almost in contact" with each other), we shift the boundaries of the domain by a small distance $\Delta_3$ taken in this work to be 0.3 Å. The final domain used for $u_{e\|}(h,\xi)$ in the numerical implementation of the tubular potential is shown as the gray area in Figure S1.

For function $\Phi(h,\zeta)$, the computational domain used in the numerical implementation of the tubular potential is schematically shown as the gray area in Figure S2. The "upper" boundary of the domain is defined by function $\zeta_{\max}(h) = \sqrt{h_{\max}^2 - h^2}$, while the "lower" boundary is defined by function $\zeta_{\min}(h)$ that is introduced in eq 23. As discussed in the text of the paper, function $\zeta_{\min}(h)$ must satisfy the conditions given by eq 24 and should have a continuous derivative.

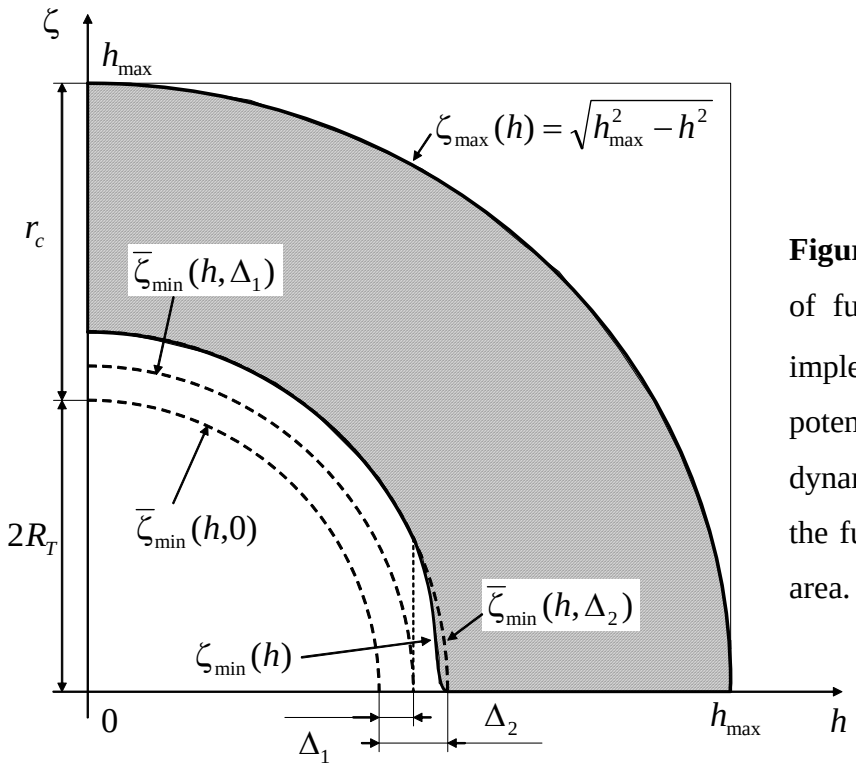


**Figure S2**. Sketch of the domain of function $\Phi(h,\zeta)$ used in the implementation of the tubular potential in the mesoscopic dynamic model. The domain of the function is shown as the gray area.

In order to define $\zeta_{\min}(h)$, we first introduce a continuous but not differentiable function defined for $h > 0$ as follows:

$$\overline{\zeta}_{\min}(h,\Delta) = \begin{cases} \sqrt{(2R_T + \Delta)^2 - h^2} & \text{if } 0 < h \le 2R_T + \Delta, \\ 0 & \text{if } h > 2R_T + \Delta, \end{cases} \tag{S1}$$

where $\Delta$ is an arbitrary positive constant. The function $\overline{\zeta}_{\min}(h,\Delta)$ has infinite derivative $d\overline{\zeta}_{\min}/dh$ at $h = 2R_T + \Delta$. Next, we introduce a differentiable function $\zeta_{\min}(h)$, which satisfies a condition $\overline{\zeta}_{\min}(h,\Delta_1) \le \zeta_{\min}(h) \le \overline{\zeta}_{\min}(h,\Delta_2)$, where $\Delta_1$ and $\Delta_2$ are positive constants that are much smaller than the equilibrium distance $r_0$ of the interatomic potential $\varphi(r)$. In calculations, we define the smooth function $\zeta_{\min}(h)$ with the help of a fifth order polynomial as follows:

$$\zeta_{\min}(h) = \overline{\zeta}_{\min}(h,\Delta_2) S_5\left(\frac{h - 2R_T - \Delta_1}{\Delta_2 - \Delta_1}\right), \tag{S2}$$

$$S_5(\tau) = H(-\tau) + H(\tau)H(1-\tau)[1 - \tau^3(6\tau^2 - 15\tau + 10)], \tag{S3}$$

where $H(\tau)$ is the Heaviside step function. The functions $\overline{\zeta}_{\min}(h,\Delta_1)$, $\overline{\zeta}_{\min}(h,\Delta_2)$, and $\zeta_{\min}(h)$ are shown schematically in Figure S2. In the calculations reported in this paper, the values of $\Delta_1$ and $\Delta_2$ are chosen to be 1 Å and 2 Å, respectively.

The evaluation of function $u_{e\|}(h,\xi)$ and its derivatives is done in this work by bi-cubic spline interpolation[S2] performed on a homogeneous Cartesian mesh that covers the domain shown in Figure S1 and is compatible with the six corners of the domain. The procedure of finding the coefficients of the spline function in this case is similar to the one used for rectangular domains.[S2] The values of $u_{e\|}(h,\xi)$ are calculated for each node of the mesh by numerical integration of eq 29. The number of quadrature points used in the integration is 128 for the cross sections of the nanotubes (angles $\phi_1$ and $\phi_2$) and 129 along the axis of the nanotube (variable $\eta$). The integration over $\eta$ is performed for interval $[\max(0, \xi - \eta_{\max}(h)), \xi + \eta_{\max}(h)]$, where $\eta_{\max}(h) = \sqrt{r_c^2 - (h - 2R_T)^2}$, since potential $\varphi(r)$ in eq 1 is equal to zero for any value of $\eta$ outside this interval. The bi-cubic spline function for $u_{e\|}(h,\xi)$ is calculated for conditions of

zero values of the appropriate second and fourth derivatives at the domain boundaries. These conditions ensure the existence and uniqueness of the interpolation function.

The function $u_{\infty\|}(h)$ is also calculated by cubic interpolation of values tabulated in a one-dimensional table. On can avoid building a separate table for $u_{\infty\|}(h)$ as the values of $u_{\infty\|}(h)$ can be obtained by bi-cubic spline interpolation from the table created for $u_{e\|}(h,\xi)$, using equation $u_{\infty\|}(h) = u_{e\|}(h, r_c)$. The bi-cubic spline interpolation, however, is more computationally expensive compared to the cubic interpolation. Therefore, we use a separate cubic spline function for $u_{\infty\|}(h)$.

The evaluation of function $\Phi(h,\zeta)$ and its derivatives is also based on bi-cubic spline interpolation. In this case, however, in order to use a conventional procedure for calculation of the coefficients of bi-cubic spline function on a Cartesian mesh of a rectangular shape, we apply a transformation of variable $\zeta$ to $\psi = [\zeta - \zeta_{\min}(h)]/[\zeta_{\max}(h) - \zeta_{\min}(h)]$, so that the domain of function $\Phi$ transforms into a rectangle $[0, h_{\max}]\times[0,1]$ for the new set of variables $(h,\psi)$. The values of function $\overline{\Phi}(h,\psi) = \Phi(h, \zeta_{\min}(h) + [\zeta_{\max}(h) - \zeta_{\min}(h)]\psi)$ are then calculated for each node of the new homogeneous rectangular Cartesian mesh by numerical integration of eq 23, with values of potential density $u_{\infty\|}(h)$ obtained by the cubic spline interpolation as discussed above. Finally, the coefficients of the bi-cubic spline function for $\overline{\Phi}(h,\psi)$ are obtained for conditions of zero values of the appropriate second and fourth derivatives on the domain boundaries. The use of function $\zeta_{\min}(h)$ in the form of eqs S2 and S3 ensures continuity of second derivatives of $\overline{\Phi}(h,\psi)$. In this case, $\overline{\Phi}(h,\psi)$ belongs to the same differentiability class as its bi-cubic spline approximation.

The size of the tables used for storing functions $u_{e\|}(h,\xi)$ and $\Phi(h,\zeta)$, as well as their derivatives, is chosen in this work to be 1001×1001. An important advantage of the bi-cubic spline interpolation is that the derivatives of the functions (that are necessary for calculation of forces) are readily available as derivatives of the spline functions. As a result, the interaction energies and forces remain consistent with each other even if a relatively small number of the mesh nodes are used in the calculations. The minimum number of values that have to be stored in the two-dimensional tables is determined in this case not by the error in the total energy

conservation in a mesoscopic dynamic simulation, but by the need to ensure a sufficient accuracy of interpolation in the regions where the derivatives of the functions are large. In contrast, the use of bi-linear interpolation in the two-dimensional tables (which is a generalization of an approach commonly used in atomistic molecular dynamics simulations, e.g. ref S1) requires a much larger number of mesh nodes in order to achieve a level of consistency between the forces and potentials that provides an acceptable accuracy of the total energy conservation. For example, we found that in order to achieve the same quality of the energy conservation in the simulation discussed in section 4, the number of mesh points has to be increased from $10^6$ to $2\times10^7$, i.e. by a factor of 20 compared to the bi-cubic spline interpolation. Storing the corresponding tables of the two functions ($\Phi(h,\zeta)$ and $u_{e\|}(h,\xi)$) and their derivatives in a computer memory would require at least $2\times3\times8\times2\times10^7 \approx 1$ Gb and would put rather stringent requirements on the computational resources needed for large-scale dynamic simulations.

The use of the bi-cubic spline interpolation for calculation of the tubular potential provides an additional benefit of eliminating the necessity to introduce an explicit smooth transition between the case of non-parallel nanotube segments described by eq 25 and the limiting case of parallel segments described by eq 9. We find that it is possible to switch directly between the two cases at a pre-defined threshold angle, i.e.

$$\breve{U}_{S\infty}(h,\alpha,\xi_1,\xi_2)=\begin{cases} U_{S\infty\|}(h,\xi_1,\xi_2), & \sin^2\alpha<\Delta_\alpha; \\ \tilde{U}_{S\infty}(h,\alpha,\xi_1,\xi_2), & \sin^2\alpha\geq\Delta_\alpha, \end{cases} \tag{S4}$$

where the constant $\Delta_\alpha$ can be as small as $10^{-6}$. Undoubtedly, this non-smooth transition introduces an additional error, which can be particularly significant in the case when the majority of nanotubes are almost parallel to each other, e.g. when they are arranged into bundles. Nevertheless, we find that in the dynamic mesoscopic simulation of a single-walled CNT sample described in section 4 this approach demonstrates an acceptable level of the total energy conservation. The drift in the total energy during the first nanosecond of the simulation does not exceed 2% of the kinetic energy of the system.

## S2. Calculation of Forces Acting on a Segment and a Nanotube

The numerical integration of the equations of motions of nanotubes in a mesoscopic dynamic simulation requires evaluation of forces acting on nanotubes. The calculation of forces involves differentiation of the interaction potential, which should be formulated in terms of position vectors that uniquely define the positions of the interacting tubes in a global system of coordinates. In this part of the Supporting Information we present the complete description of the calculation of forces acting on nanotubes that interact with each other through the tubular potential defined by eqs 25 and 39.

The position of a finite straight segment of a nanotube is defined in a natural way by the position vectors of its ends, $\mathbf{r}_1$ and $\mathbf{r}_2$ (Figure S3). In order to specify the position of semi-infinite or infinitely-long straight nanotube, one or two points at the tube axis can be chosen arbitrarily. In particular, the position of a semi-infinite straight nanotube can be specified by the position vectors of its end $\mathbf{q}_e$ and any other arbitrary point located at the axis of the nanotube. Here, however, we use an alternative way to specify the positions of semi-infinite nanotubes, which simplifies the application of the potential in the case of curved nanotubes. Namely, the position of a semi-infinite nanotube is defined by two arbitrary points located at the axis of the nanotube with position vectors $\mathbf{p}_1$ and $\mathbf{p}_2$, as well as by a coordinate $\rho_e$ of the nanotube end. The coordinate $\rho_e$ is defined along the axis of the semi-infinite nanotube with respect to the midpoint of the vector connecting points $\mathbf{p}_1$ and $\mathbf{p}_2$, so that the position of the end of the nanotubes can be expressed as

$$\mathbf{q}_e = \mathbf{p} - \rho_e \mathbf{m}, \tag{S5}$$

where $\mathbf{p} = (1/2)(\mathbf{p}_2 + \mathbf{p}_1)$ and $\mathbf{m} = (\mathbf{p}_2 - \mathbf{p}_1)/|\mathbf{p}_2 - \mathbf{p}_1|$ is the unit vector defining the direction of the nanotube (Figure S3). Note that the position vectors $\mathbf{r}_1$, $\mathbf{r}_2$, $\mathbf{p}_1$ and $\mathbf{p}_2$ are defined in a global system of coordinates and are suitable for describing the dynamic behavior of an ensemble of interacting nanotubes.

In order to decrease the number of different geometrical cases to be considered, we restrict further consideration by the following condition,

$$|\mathbf{p}_2 - \mathbf{q}_e| > |\mathbf{p}_1 - \mathbf{q}_e|, \tag{S6}$$

which implies that point $\mathbf{p}_1$ is located between $\mathbf{q}_e$ and $\mathbf{p}_2$. This condition can always be satisfied by choosing an appropriate numbering of points $\mathbf{p}_1$ and $\mathbf{p}_2$.

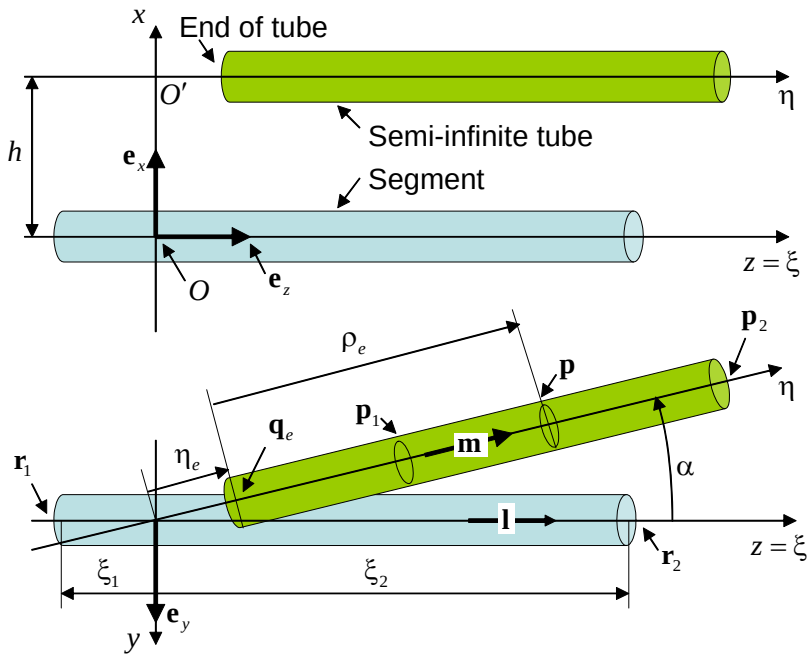


**Figure S3.** Schematic sketch illustrating the introduction of local Cartesian coordinates $Oxyz$, geometric parameters describing the relative positions of a nanotube segment and a semi-infinite nanotube, and position vectors defining the positions of the segment and nanotube in a global system of coordinates. The side and top views are shown in the upper and lower panels, respectively.

The geometric parameters $h$, $\alpha$, $\xi_1$, $\xi_1$ and $\eta_e$ that define the tubular potentials $\tilde{U}_{S\infty}$ and $\tilde{U}_{Se}$ (eqs 25 and 39) are functions of position vectors $\mathbf{r}_1$, $\mathbf{r}_2$, $\mathbf{p}_1$, $\mathbf{p}_2$ and coordinate $\rho_e$, i.e.

$$h = h(\mathbf{r}_1,\mathbf{r}_2,\mathbf{p}_1,\mathbf{p}_2),\quad \alpha = \alpha(\mathbf{r}_1,\mathbf{r}_2,\mathbf{p}_1,\mathbf{p}_2),\quad \xi_1 = \xi_1(\mathbf{r}_1,\mathbf{r}_2,\mathbf{p}_1,\mathbf{p}_2),\quad \xi_2 = \xi_2(\mathbf{r}_1,\mathbf{r}_2,\mathbf{p}_1,\mathbf{p}_2), \qquad \text{(S7)}$$

$$\eta_e = \eta_e(\mathbf{r}_1,\mathbf{r}_2,\mathbf{p}_1,\mathbf{p}_2,\rho_e). \qquad \text{(S8)}$$

The functional forms of these dependences are derived in sub-section S2.1.

By inserting eqs S7 and S8 into the right parts of eqs 25 and 39, one can express the tubular potential through the position vectors of the interacting nanotubes, i.e. in the form $\tilde{U}_{S\infty} = \tilde{U}_{S\infty}(\mathbf{r}_1,\mathbf{r}_2,\mathbf{p}_1,\mathbf{p}_2)$ and $\tilde{U}_{Se} = \tilde{U}_{Se}(\mathbf{r}_1,\mathbf{r}_2,\mathbf{p}_1,\mathbf{p}_2,\rho_e)$. The corresponding forces, obtained by differentiation of these potentials, are presented in sub-sections S2.2 and S2.3 in a form suitable for straightforward implementation in a computer code.

## S2.1. Calculation of Geometric Parameters

To enable the calculation of forces, the geometric parameters $h$, $\alpha$, $\xi_1$, $\xi_1$ and $\eta_e$ that specify the relative position of a segment and a nanotube in a local system of coordinates should be expressed through the position vectors $\mathbf{r}_1$, $\mathbf{r}_2$, $\mathbf{p}_1$, $\mathbf{p}_2$ and the coordinate $\rho_e$ defining the positions of the segment and the nanotube in the global system of coordinates.

Before considering the infinitely-long and semi-infinite nanotubes, it is convenient to start from a more general case of two cylindrical segments of finite lengths, with ends of the segments defined by position vectors $\mathbf{r}_1$, $\mathbf{r}_2$, $\mathbf{p}_1$, and $\mathbf{p}_2$ (Figure S4).

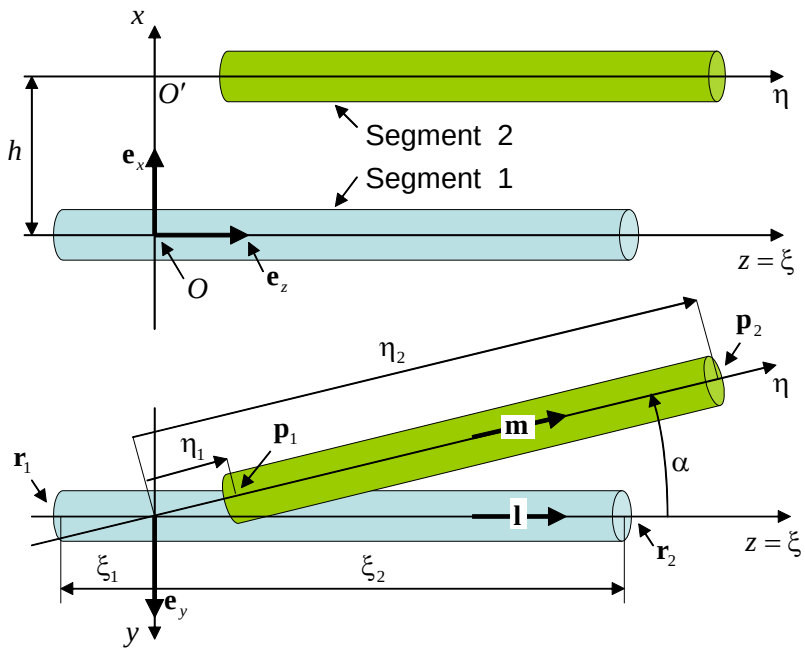


**Figure S4.** Schematic sketch illustrating the local Cartesian coordinates $Oxyz$, geometric parameters describing the relative positions of two nanotube segments, and position vectors defining the positions of the segments in a global system of coordinates. The side and top views are shown in the upper and lower panels, respectively.

The description of this system can be simplified by introduction of points $\mathbf{r}$ and $\mathbf{p}$ in the middle of the segments, a vector defining the relative position of the two midpoints $\Delta\mathbf{r}$, the direction vectors of the two segments $\mathbf{l}$ and $\mathbf{m}$, the lengths of segments $L_r$ and $L_p$, and cosine of the angle between the segments' axes $\Psi$:

$$\mathbf{r} = \frac{1}{2}(\mathbf{r}_2 + \mathbf{r}_1), \quad \mathbf{p} = \frac{1}{2}(\mathbf{p}_2 + \mathbf{p}_1), \tag{S9}$$

$$\Delta\mathbf{r} = \mathbf{p} - \mathbf{r}, \quad L_r = |\mathbf{r}_2 - \mathbf{r}_1|, \quad L_p = |\mathbf{p}_2 - \mathbf{p}_1|, \quad \mathbf{l} = \frac{\mathbf{r}_2 - \mathbf{r}_1}{L_r}, \quad \mathbf{m} = \frac{\mathbf{p}_2 - \mathbf{p}_1}{L_p}, \quad \Psi = \mathbf{l} \cdot \mathbf{m}. \tag{S10}$$

First we consider the case of non-parallel axes ($|\Psi| \neq 1$). The shortest distance between the axes of the segments is realized along the vector $\Delta\bar{\mathbf{r}}$ connecting points $O$ and $O'$ that have the position vectors $\bar{\mathbf{r}}$ and $\bar{\mathbf{p}}$, respectively. This vector $\Delta\bar{\mathbf{r}}$ can be expressed through the geometric parameters defined by eqs S9 and S10 as follows:

$$\bar{\mathbf{r}} = \mathbf{r} + \tau_r \mathbf{l}, \quad \bar{\mathbf{p}} = \mathbf{p} + \tau_p \mathbf{m}, \tag{S11}$$

$$\tau_r = \frac{\Delta\mathbf{r} \cdot (\mathbf{l} - \Psi\mathbf{m})}{1 - \Psi^2}, \qquad \tau_p = \frac{\Delta\mathbf{r} \cdot (\Psi\mathbf{l} - \mathbf{m})}{1 - \Psi^2}, \tag{S12}$$

$$\Delta\bar{\mathbf{r}} = \bar{\mathbf{p}} - \bar{\mathbf{r}}. \tag{S13}$$

Then the basis vectors $\mathbf{e}_x$, $\mathbf{e}_y$, and $\mathbf{e}_z$ of the Cartesian coordinates $Oxyz$ in Figure S4 can be defined as

$$\mathbf{e}_x = \frac{\Delta\bar{\mathbf{r}}}{h}, \qquad \mathbf{e}_z = \mathbf{l}, \qquad \mathbf{e}_y = \mathbf{e}_z \times \mathbf{e}_x. \tag{S14}$$

It allows to express the distance $h$ and angle $\alpha$ between the axes of the segments and the coordinates $\xi_i$ and $\eta_i$ ($i$ = 1,2) of the segments' ends as follows

$$h = |\Delta\bar{\mathbf{r}}|, \qquad \alpha = \begin{cases} \arccos\Psi, & \text{if } \mathbf{m} \cdot \mathbf{e}_y < 0; \\ 2\pi - \arccos\Psi, & \text{otherwise,} \end{cases} \tag{S15}$$

$$\xi_i = (\mathbf{r}_i - \bar{\mathbf{r}}) \cdot \mathbf{l} = (\mathbf{r}_i - \mathbf{r}) \cdot \mathbf{l} - \tau_r, \tag{S16}$$

$$\eta_i = (\mathbf{p}_i - \bar{\mathbf{p}}) \cdot \mathbf{m} = (\mathbf{p}_i - \mathbf{p}) \cdot \mathbf{m} - \tau_p. \tag{S17}$$

Thus, eqs S14-S17 enable calculation of all the geometrical parameters of a pair of segments based on the position vectors defining the positions of the segments in a global system of coordinates. These results can be easily adopted to the cases where one of the segments is replaced by an infinitely long or a semi-infinite nanotube.

In the case of an infinitely long tube, it is sufficient to omit eq S17.

In the case of a semi-infinite nanotube, the coordinate $\eta_e$ of the end of the nanotube with respect to the point $O'$ can be expressed through the coordinate $\rho_e$ satisfying eq S5 and parameter $\tau_p$ defined by eq S12 as follows:

$$\eta_e = (\mathbf{q}_e - \bar{\mathbf{p}}) \cdot \mathbf{m} = -\rho_e - \tau_p . \qquad \text{(S18)}$$

In the case where the axes of a segment and a semi-infinite nanotube are parallel to each other ($|\Psi| = 1$), the origin $O$ of the local system of coordinates can be chosen arbitrarily along the axis of the segment. We chose the position of the origin $O$ so that the axis $Ox$ goes through the end of the semi-infinite nanotube. In this case, $\sin\alpha = 0$ and all other geometrical parameters can be calculated with the corresponding eqs S11, S13-S18, where $\tau_r$ and $\tau_p$ are defined as

$$\tau_r = \Delta\mathbf{r} \cdot \mathbf{l} - \rho_e \mathbf{m} \cdot \mathbf{l}, \qquad \tau_p = -\rho_e \qquad \text{(S19)}$$

instead of eqs S12.

Thus, the system of eqs S9-S19 provides the functional dependence of the geometric parameters $h$, $\alpha$, $\xi_1$, $\xi_1$ and $\eta_e$ defining the relative positions of a nanotube segment and a finite, semi-infinite, or infinite nanotube from the position vectors defining the positions of the segment and the nanotube in a global system of coordinates. These equations, therefore, represent a specific form of eqs S7 and S8.

Eqs S10 and S12-S19 depend only on the relative positions of points $\mathbf{r}_1$, $\mathbf{r}_2$, $\mathbf{p}_1$, and $\mathbf{p}_2$ (nodes in the mesoscopic model of nanotubes described in Section 4 of the paper). Therefore, these equations expressing the local geometric parameters through the positions of nodes, as well as the procedures for the calculation of forces presented in the following sections, can be readily adopted for simulations performed with periodic boundary conditions, which exploit the minimum image convention (e.g., see Ref. S3). In the case of the periodic boundary conditions, the minimum image convention is applied to the vector subtraction operations in the right parts of eqs S10 and S13.

### S2.2. Calculation of Forces in the Case of an Infinitely Long Nanotube

In this section, we derive expressions for forces arising from the interaction between a segment and an infinitely long nanotube. The interaction between the segment and the nanotube is described by the tubular potential $\tilde{U}_{S\infty}$ given by eq 25. The positions of the ends of the segment are defined by position vectors $\mathbf{r}_1$ and $\mathbf{r}_2$, and the position of the nanotube is specified

by the position vectors $\mathbf{p}_1$ and $\mathbf{p}_2$. The corresponding geometric parameters $h$, $\alpha$, $\xi_1$, and $\xi_1$ can be calculated from these global position vectors as described in the previous section.

The straightforward way to calculate forces $\mathbf{F}_{\infty i}$ acting on the ends $\mathbf{r}_i$ of the segment is to insert eqs S7 into the right part of eq 25 and then find the forces by calculating the gradient of the potential with respect to the position vectors, $\mathbf{F}_{\infty i} = -\partial \tilde{U}_{S\infty} / \partial \mathbf{r}_i$. Due to the complex structure of the geometrical relations in eqs S7, the implementation of this method involves rather cumbersome derivations.

A more simple and elegant derivation of forces is only possible under assumption of $\Gamma(h,\alpha) = \Omega(\alpha) = 1$. In this case, the potential density is given by eq 11 and is a function of the distance between the point on the axis of the segment and the axis of the tube ($\sqrt{h^2 + (\xi \sin\alpha)^2}$) only. The potential density at any given point along the axis of the segment is not affected by any translations or rotations of the segment that do not affect the distance between this point to the axis of the nanotube. This observation enables calculation of the distribution of forces along the segment by direct differentiation of eq 11, which is relatively easy to do. Integration of the force distribution along the segment axis can then be used to evaluate forces acting on the ends of the segment. This derivation of forces can be used as an intermediate step, for testing the consistency of forces and energies in the mesoscopic model. It is unlikely, however, that this simple approach can be extended to the general case of the potential density described by eq 12, as this density explicitly depends on the orientation of the entire segment with respect to the nanotube. In this case we did not find any alternatives to the calculation of forces using the straightforward approach described above, i.e. by evaluation of $\mathbf{F}_{\infty i} = -\partial \tilde{U}_{S\infty} / \partial \mathbf{r}_i$. Omitting all auxiliary calculations, below we present only the final result of the derivations.

We assume that the derivatives of all functions entering eq 25 are calculated and tabulated for computationally efficient evaluation in the course of a dynamic simulation. To make the expressions for the force components more compact, we introduce the following notation for these functions and their derivatives:

$$\overline{\Gamma} = \Gamma(h,\alpha), \quad \overline{\Gamma}_h = \frac{\partial \Gamma}{\partial h}(h,\alpha), \quad \overline{\Gamma}_\alpha = \frac{\partial \Gamma}{\partial \alpha}(h,\alpha), \tag{S20}$$

$$\overline{\Omega} = \Omega(\alpha), \quad \overline{\Omega}_\alpha = \frac{d\Omega}{d\alpha}(\alpha), \tag{S21}$$

$$\overline{\Phi}_i = \Phi(h,\zeta_i), \quad \overline{\Phi}_{ih} = \frac{\partial\Phi}{\partial h}(h,\zeta_i), \quad \overline{\Phi}_{i\zeta} = \frac{\partial\Phi}{\partial\zeta}(h,\zeta_i), \quad i = 1,2, \tag{S22}$$

where $\zeta_i = \xi_i\overline{\Omega}\sin\alpha$.

In the local Cartesian coordinates (Figure S3), the forces $\mathbf{F}_{\infty i}$ acting on the ends of the segment can be represented in the form

$$\mathbf{F}_{\infty i} = F_{\infty ix}\mathbf{e}_x + F_{\infty iy}\mathbf{e}_y + F_{\infty iz}\mathbf{e}_z, \quad i = 1,2, \tag{S23}$$

and the components of forces can be calculated as follows

$$F_{\infty 1x} = \frac{1}{L}\left[\xi_2\frac{\partial\overline{U}}{\partial h} - \frac{h\overline{\Gamma}}{\sin^2\alpha}\left(\overline{\Phi}_{2\zeta} - \overline{\Phi}_{1\zeta}\right)\right], \quad F_{\infty 2x} = \frac{1}{L}\left[-\xi_1\frac{\partial\overline{U}}{\partial h} + \frac{h\overline{\Gamma}}{\sin^2\alpha}\left(\overline{\Phi}_{2\zeta} - \overline{\Phi}_{1\zeta}\right)\right], \tag{S24}$$

$$F_{\infty 1y} = \frac{1}{L}\left[\frac{\partial\overline{U}}{\partial\alpha} - \xi_2\overline{\Gamma}\frac{\cos\alpha}{\sin\alpha}\left(\overline{\Phi}_{2\zeta} - \overline{\Phi}_{1\zeta}\right)\right], \quad F_{\infty 2y} = \frac{1}{L}\left[-\frac{\partial\overline{U}}{\partial\alpha} + \xi_1\overline{\Gamma}\frac{\cos\alpha}{\sin\alpha}\left(\overline{\Phi}_{2\zeta} - \overline{\Phi}_{1\zeta}\right)\right], \tag{S25}$$

$$F_{\infty 1z} = \overline{\Gamma}\overline{\Phi}_{1\zeta}, \quad F_{\infty 2z} = -\overline{\Gamma}\overline{\Phi}_{2\zeta}, \tag{S26}$$

where

$$\frac{\partial\overline{U}}{\partial h} = \frac{\overline{\Gamma}_h}{\overline{\Gamma}}\overline{U} + \frac{\overline{\Gamma}}{\overline{\Omega}\sin\alpha}\left(\overline{\Phi}_{2h} - \overline{\Phi}_{1h}\right), \tag{S27}$$

$$\frac{\partial\overline{U}}{\partial\alpha} = \frac{\overline{\Gamma}_\alpha}{\overline{\Gamma}}\overline{U} + \frac{\left(\overline{\Omega}_\alpha\sin\alpha + \overline{\Omega}\cos\alpha\right)}{\overline{\Omega}\sin\alpha}\left[\overline{\Gamma}\left(\xi_2\overline{\Phi}_{\zeta 2} - \xi_1\overline{\Phi}_{\zeta 1}\right) - \overline{U}\right], \tag{S28}$$

$$\overline{U} = \frac{\overline{\Gamma}\left(\overline{\Phi}_2 - \overline{\Phi}_1\right)}{\overline{\Omega}\sin\alpha}, \quad L = |\mathbf{r}_2 - \mathbf{r}_1| = \xi_2 - \xi_1. \tag{S29}$$

In the case of $\sin\alpha = 0$, eqs S24 and S25 as well as the potential itself (eq 25) have indeterminate forms. Nevertheless, by applying l'Hôpital's rule to eqs S24 and S25 and taking into account eq 14, one can prove that

$$\lim_{\sin\alpha\to 0} F_{\infty ix} = -\frac{\xi_2 - \xi_1}{2}\frac{\partial u_{\infty\|}}{\partial h}(h) = -\frac{\partial U_{S\infty\|}}{\partial h}, \quad \lim_{\sin\alpha\to 0} F_{\infty iy} = 0. \tag{S28}$$

Considering a limiting case of eqs S26 one can also show that

$$\lim_{\sin\alpha\to 0} F_{\infty 1z} = u_{\infty\|}(h) = -\frac{\partial U_{S\infty\|}}{\partial \xi_1}, \qquad \lim_{\sin\alpha\to 0} F_{\infty 2z} = -u_{\infty\|}(h) = -\frac{\partial U_{S\infty\|}}{\partial \xi_2}. \tag{S29}$$

Eqs S28 and S29 imply that eqs S24-S26 approach the correct values in the limit of parallel tubes.

For the calculation of forces $\mathbf{P}_{\infty i} = -\partial U_{S\infty} / \partial \mathbf{p}_i$ applied to the points $\mathbf{p}_i$ of the nanotube, one can use the laws of momentum and angular momentum conservation that should be satisfied in a system that consists of a segment and a nanotube experiencing only the internal forces. The conservation of momentum and angular momentum results in the following equations:

$$\mathbf{P}_{\infty 1} + \mathbf{P}_{\infty 2} = -\mathbf{F}, \quad (\mathbf{p}_1 - \mathbf{p}) \times \mathbf{P}_{\infty 1} + (\mathbf{p}_2 - \mathbf{p}) \times \mathbf{P}_{\infty 2} = -\mathbf{M}, \tag{S30}$$

where

$$\mathbf{F} = \mathbf{F}_{\infty 1} + \mathbf{F}_{\infty 2} \quad \text{and} \quad \mathbf{M} = (\mathbf{r}_1 - \mathbf{p}) \times \mathbf{F}_{\infty 1} + (\mathbf{r}_2 - \mathbf{p}) \times \mathbf{F}_{\infty 2}. \tag{S31}$$

are the total force $\mathbf{F}$ and torque $\mathbf{M}$ calculated with respect to the point $\mathbf{p} = (1/2)(\mathbf{p}_1 + \mathbf{p}_2)$.

In general, for two arbitrary rigid bodies, eqs S30 have non-unique solutions, since if $\mathbf{P}_{\infty 1}$ and $\mathbf{P}_{\infty 2}$ is a solution, then vectors $\mathbf{P}_{\infty 1} + a\mathbf{m}$ and $\mathbf{P}_{\infty 2} - a\mathbf{m}$ with arbitrary $a$ also satisfy eqs S31 (here $\mathbf{m} = (\mathbf{p}_2 - \mathbf{p}_1)/|\mathbf{p}_2 - \mathbf{p}_1|$). It is obvious from symmetry reasons, however, that the tubular potential for an infinitely long tube, $\tilde{U}_{S\infty}(h, \alpha, \xi_1, \xi_2)$, can not produce forces that act along the axis of the nanotube, i.e. $\mathbf{P}_i \cdot \mathbf{m} = 0$ (one can also prove the validity of this equations by direct differentiation of eq 25). This additional requirement results in the existence of a unique solution of eqs S30, which has the following form:

$$\mathbf{P}_{\infty 1} = -\frac{\mathbf{F}}{2} + \frac{\mathbf{M} \times \mathbf{m}}{|\mathbf{p}_2 - \mathbf{p}_1|}, \quad \mathbf{P}_{\infty 2} = -\frac{\mathbf{F}}{2} - \frac{\mathbf{M} \times \mathbf{m}}{|\mathbf{p}_2 - \mathbf{p}_1|}. \tag{S32}$$

Eqs S24-S29, S31, and S32 provide a straightforward algorithm for calculation of forces acting between a segment and an infinitely long straight tube.

### S2.3. Calculation of Forces in the Case of a Semi-Infinite Nanotube

In this section, we derive expressions for forces arising from the interaction between a segment and a semi-infinite nanotube. The interaction between the segment and the nanotube is described by the tubular potential $\tilde{U}_{Te}$ given by eq 39. The positions of the ends of the segment

are defined by position vectors $\mathbf{r}_1$ and $\mathbf{r}_2$, and the position of the nanotube is specified by the position vectors $\mathbf{p}_1$ and $\mathbf{p}_2$, as well as by the coordinate of the nanotube end $\rho_e$ that satisfies eq S5. The corresponding geometric parameters $h$, $\alpha$, $\xi_1$, $\xi_1$, and $\eta_e$ can be calculated from the global position vectors and coordinate $\rho_e$ as described in section S2.1.

Similarly to the derivations discussed for the infinitely long nanotube in the previous section, forces $\mathbf{F}_{ei}$ acting on the ends $\mathbf{r}_i$ of the segment are calculated here by inserting eqs S7 and S8 into the right part of eq 39 and calculating the gradients of the potential with respect to the position vectors. Omitting all auxiliary calculations, below we present only the final equations for the components of forces $\mathbf{F}_{ei}$ in the local Cartesian coordinates (Figure S3):

$$\mathbf{F}_{ei} = -\frac{\tilde{U}_{Se}}{\partial \mathbf{r}_i} = F_{eix}\mathbf{e}_x + F_{eiy}\mathbf{e}_y + F_{eiz}\mathbf{e}_z, \quad i = 1,2. \tag{S33}$$

We assume that the derivatives of all functions entering the right part of eq 39 are calculated and tabulated for computationally efficient evaluation in the course of a dynamic simulation. To make the expressions for the force components more compact, we use the notations defined by eqs S20 and S21, and introduce the following additional notations:

$$\overline{\Theta} = \Theta(\alpha), \quad \overline{\Theta}_\alpha = \frac{d\Theta}{d\alpha}(\alpha), \tag{S34}$$

$$\overline{u}_{(n)} = c_{(n)} u_{e\|}\left(\overline{h}_{(n)}, \overline{\vartheta}_{(n)}\right), \quad \overline{u}_{h(n)} = \frac{c_{(n)}}{\overline{h}_{(n)}} \frac{\partial u_{e\|}}{\partial h}\left(\overline{h}_{(n)}, \overline{\vartheta}_{(n)}\right), \quad \overline{u}_{\xi(n)} = c_{(n)} \frac{\partial u_{e\|}}{\partial \xi}\left(\overline{h}_{(n)}, \overline{\vartheta}_{(n)}\right), \tag{S35}$$

$$J_h = \Delta\xi\overline{\Gamma}\sum_{n=0}^{N_\xi - 1}\overline{u}_{h(n)}, \quad J_{h1} = \Delta\xi\overline{\Gamma}\sum_{n=0}^{N_\xi - 1}\overline{\xi}_{(n)}\overline{u}_{h(n)}, \quad J_{h2} = \Delta\xi\overline{\Gamma}\sum_{n=0}^{N_\xi - 1}\overline{\xi}_{(n)}^2\overline{u}_{h(n)}, \tag{S36}$$

$$J_\xi = \Delta\xi\overline{\Gamma}\sum_{n=0}^{N_\xi - 1}\overline{u}_{\xi(n)}, \quad J_{\xi 1} = \Delta\xi\overline{\Gamma}\sum_{n=0}^{N_\xi - 1}\xi_{(n)}\overline{u}_{\xi(n)}, \tag{S37}$$

$$\overline{U} = \Delta\xi\overline{\Gamma}\sum_{n=0}^{N_\xi - 1}\overline{u}_{(n)}, \quad \overline{U}_h = \frac{\overline{\Gamma}_h}{\overline{\Gamma}}\overline{U} + hJ_h, \tag{S38}$$

$$\overline{U}_\alpha = \frac{\overline{\Gamma}_\alpha}{\overline{\Gamma}}\overline{U} + \overline{\Omega}\sin\alpha\left(\overline{\Omega}_\alpha\sin\alpha + \overline{\Omega}\cos\alpha\right)J_{h2} - \sin\alpha J_{\xi 1} - \overline{\Theta}_\alpha\eta_e J_\xi, \tag{S39}$$

$$C_x = h\left[\overline{\Omega}^2 J_{h1} + \cos\alpha \frac{1-\overline{\Theta}}{\sin^2\alpha} J_\xi\right], \quad C_y = \cos\alpha \sin\alpha \overline{\Omega}^2 J_{h1} + \left(\frac{1-\overline{\Theta}}{\sin\alpha} - \sin\alpha\right) J_\xi, \tag{S40}$$

$$C_{z1} = \overline{\Omega}^2 \sin^2\alpha J_{h1} + \cos\alpha J_\xi, \quad C_{z2} = \overline{\Omega}^2 \sin^2\alpha J_{h2} + \cos\alpha J_{\xi 1}, \tag{S41}$$

$$L = \xi_2 - \xi_1, \quad c_{(n)} = \begin{cases} 1/2, & \text{if } n = 0 \text{ or } n = N_\xi - 1; \\ 1, & \text{otherwise.} \end{cases} \tag{S42}$$

Then the components of $\mathbf{F}_{ei}$ can be calculated as follows

$$F_{e1x} = \frac{\xi_2 \overline{U}_h - C_x}{L}, \quad F_{e2x} = \frac{C_x - \xi_1 \overline{U}_h}{L}, \tag{S43}$$

$$F_{e1y} = \frac{\overline{U}_\alpha - \xi_2 C_y}{L}, \quad F_{e2y} = \frac{\xi_1 C_y - \overline{U}_\alpha}{L}, \tag{S44}$$

$$F_{e1z} = \frac{C_{z2} + \overline{U} - \xi_2 C_{z1}}{L}, \quad F_{e2z} = \frac{\xi_1 C_{z1} - C_{z2} - \overline{U}}{L}. \tag{S45}$$

The values of $\overline{u}_{h(n)}$ can be calculated from eqs S35 if arguments $\overline{h}_{(n)}$ and $\overline{\vartheta}_{(n)}$ are within the domain of function $u_{e\|}(h,\xi)$ (see Figure S1 and the corresponding discussion in the text) and, additionally, $\overline{h}_{(n)} > 0$. The condition $\overline{h}_{(n)} = 0$ implies that $h = 0$. In this case, from the symmetry arguments, $u_{e\|}(h,\xi)$ should also satisfy the condition

$$\left.\frac{\partial u_{e\|}}{\partial h}\right|_{h=0} = 0. \tag{S46}$$

Then one can prove that eqs S35-S45 can be used for force calculation even for $\overline{h}_{(n)} = 0$, if $\overline{u}_{h(n)}$ is replaced by zero in this case.

If $\Theta(\alpha)$ is defined by eq 35, then $\left(1-\overline{\Theta}\right)/\sin^2\alpha$ and $\left(1-\overline{\Theta}\right)/\sin\alpha$ in eqs S40 can be replaced by $C_\Theta$ and $C_\Theta \sin\alpha$, correspondingly. In this case none of the equations for force calculation has indeterminate form at $\sin\alpha = 0$.

The forces applied to the semi-infinite nanotube interacting with the segment can be defined as follows

$$\mathbf{P}_{ei} = -\frac{\partial \tilde{U}_{Se}}{\partial \mathbf{p}_i}, \quad Q_{ee} = -\frac{\partial \tilde{U}_{Se}}{\partial \rho_e}, \tag{S47}$$

where $\mathbf{P}_{ei}$ is the force applied at point $\mathbf{p}_i$ and scalar $Q_{ee}$ is equal to the force applied to the nanotube end and acting along the nanotube axis in the direction opposite to the direction of vector $\mathbf{m} = (\mathbf{p}_2 - \mathbf{p}_1)/|\mathbf{p}_2 - \mathbf{p}_1|$. One can conclude from eq S18 that $\partial \eta_e / \partial \rho_e = -1$, so that the force $Q_{ee}$ can be easily found by differentiation of eq 39:

$$Q_{ee} = -\overline{\Theta} J_\xi . \tag{S48}$$

Forces $\mathbf{P}_{ei}$ can be found by following an approach described in section S2.2 for the corresponding forces $\mathbf{P}_{\infty i}$ acting on an infinitely long tube, using the conservation laws for momentum and angular momentum. Contrary to the case of the infinitely long tube, for a semi-infinite tube the total force acting along the tube axis is not equal to zero, i.e. $(\mathbf{P}_{e1} + \mathbf{P}_{e2}) \cdot \mathbf{m} \neq 0$. At the same time, one can prove that $\mathbf{P}_{e1} \cdot \mathbf{m} = \mathbf{P}_{e2} \cdot \mathbf{m}$. Physically, the last condition is obvious because (i) the force components acting along the tube axis appear only due to the presence of the tube's end and (ii) the forces $\mathbf{P}_{ei}$ are defined by eqs S47 as partial derivatives at a constant distance $\rho_e$. The latter observation implies that the identical displacements of any of the two points $\mathbf{p}_i$ along the nanotube axis result in the identical changes in the position of the nanotube's end $\mathbf{q}_e$ with respect to the position of the segment defined by points $\mathbf{p}_1$ and $\mathbf{p}_2$. Therefore, the corresponding components of forces should be equal to each other.

The condition $\mathbf{P}_{e1} \cdot \mathbf{m} = \mathbf{P}_{e2} \cdot \mathbf{m}$ reduces the equations for $\mathbf{P}_{ei}$ to the form that is completely analogous to eqs S32, i.e.

$$\mathbf{P}_{e1} = -\frac{\mathbf{F}}{2} + \frac{\mathbf{M} \times \mathbf{m}}{|\mathbf{p}_2 - \mathbf{p}_1|}, \quad \mathbf{P}_{e2} = -\frac{\mathbf{F}}{2} - \frac{\mathbf{M} \times \mathbf{m}}{|\mathbf{p}_2 - \mathbf{p}_1|}, \tag{S49}$$

where

$$\mathbf{F} = \mathbf{F}_{e1} + \mathbf{F}_{e2}, \quad \mathbf{M} = (\mathbf{r}_1 - \mathbf{p}) \times \mathbf{F}_{e1} + (\mathbf{r}_2 - \mathbf{p}) \times \mathbf{F}_{e2}. \tag{S50}$$

Eqs S36-S45 and S48-S50 provide a straightforward algorithm for calculation of forces acting between a segment and a semi-infinite straight tube.

**References for the Supporting Information**

(S1) Wolff, D.; Rudd, W. G. Comput. Phys. Commun. **1999**, *120*, 20.

(S2) Marchuk, G. I. *Methods of numerical mathematics*; 2nd ed.; Springer-Verlag: New York, 1982.

(S3) Allen, M.P., Tildesley, D.J. *Computer simulation of liquids.* Clarendon Press, Oxford, 1987.